Nonlocal Response of Turbulent Plasma Transport in Tokamak Core on Fast Changes of Power Input

V.P. Pastukhov 1), N.V. Chudin 1)

1) RRC "Kurchatov Institute", 123182 Moscow, Russian Federation

E-mail contact of main author: past@nfi.kiae.ru

Abstract. Nonlocal response of low-frequency (LF) turbulence and the associated anomalous cross-field plasma transport to fast changes of power input in tokamak core plasmas is simulated and analyzed. Results of four different scenarios are discussed. Basic scenario (a) illustrates plasma confinement regime in tokamak T-10 with steady off-axis ECR heating. Two other scenarios correspond to rather quiet sawtooth-free regimes, in which the same ECR power is turned on/off or partially switched over closer to the plasma edge in particular moments of time. The simulations have shown fast (within 200-300μs) reduction (enhancement) of anomaly heat fluxes at all plasma radii after the corresponding ECR power changes in both scenarios. Scenario (d) illustrates the nonlocal response of the LF turbulence and the heat transport to presence of sawtooth oscillations.

1. Introduction

Anomalous transport of particles and energy is one of the crucial problems in magnetic plasma confinement for fusion. In most theoretical papers anomalous transport is associated with plasma fluctuations driven by various kinds of drift instabilities. Due to relatively small transverse scales of the fluctuations, the anomalous transport is conventionally discussed in terms of diffusion approximation with local transport coefficients. At the same time, many recent experiments have shown that the low-frequency (LF) turbulence and the associated anomalous cross-field plasma transport observed in various magnetic confinement systems with different magnetic field topologies and plasma parameters (tokamaks [1-3], stellarators [4,5], tandem mirrors [6,7], etc.) exhibit rather common features, which cannot be appropriately described in terms of diffusion approximation with local transport coefficients. Direct computer simulation of nonlinear plasma dynamics seems to be more appropriate method for the theoretical study of such LF turbulence and the resulting intermittent non-diffusive transport in magnetized plasmas. Contrary to simulations conventionally based on the gyrokinetic approach, we suggest simulations based on simpler adiabatically-reduced MHD-like model. Our previous investigations [8-12] have shown that such simulations can provide a quite good qualitative and quantitative agreement with many experiments.

This paper presents results of simulations of LF plasma turbulence and the associated anomalous cross-field plasma transport in tokamak core. The simulations continue our previous theoretical study of turbulence and non-diffusive transport in magnetized plasmas [8-13] and demonstrate a nonlocal response of the LF-turbulence and transport to fast changes of power input in the tokamak core. Plasma confinement regime in tokamak T-10 with off-axis ECR heating was chosen as a basic simulation regime (a). Two other simulation scenarios correspond to rather quiet sawtooth-free regimes, in which ECR power is turned on/off (scenario (c)) or radially redistributed (scenario (b)) in particular moments of time. Scenario (d) corresponds to regime with on-axis ECR heating which results in a sawtooth activity.

The basic dynamical model is briefly discussed in Section 2. Section 3 presents the results of computer simulations of LF-turbulence and transport in transient regimes in application to tokamak T-10 conditions. Brief summary is given in Section 4.

2. Basic dynamic model of nonlinear turbulent plasma convection and transport

General principles of the proposed turbulent transport model were discussed in details in our previous papers [8-13]. For application to tokamaks we assume that the plasma is self-consistently maintained near a turbulent-relaxed state which is marginally stable (MS) against an interchange pressure-driven mode in axisymmetric system with nested toroidal magnetic surfaces. The MS-state is determined by the condition $S = pU^{\gamma} = \text{const}$. Here p is the total plasma pressure; $U(\psi) = dV(\psi)/2\pi d\psi = \oint dl / B_p$ is the specific flux tube volume; γ is the adiabatic exponent, which characterizes the plasma compressibility; the poloidal magnetic flux ψ and the toroidal angle φ are used as the flux coordinates; S is a single-valued function of plasma entropy in the specific volume U. The poloidal flux ψ is normalized to present the poloidal field as $\mathbf{B}_p = [\nabla\psi \times \nabla\varphi]$. The mechanism of anomalous transport is based on competition between dissipative and ideal processes. In this case plasma heating and background thermal conductivity distort the initial pressure profile making it a weakly unstable, while the instability induces and maintains quasi-2D nonlinear convection, which tends to restore the MS pressure profile and results in anomalous non-diffusive plasma transport. Below we discuss simulations for tokamaks with large aspect ratios ($A = R/a >> 1$) and almost circular poloidal cross-sections (in particular, tokamak T-10). Such simulations can be performed in a framework of simplified cylindrical model, in which the system is periodic along z-axis with the period $2\pi R$ and the effective "toroidal" angle is defined as $\varphi = z/R$.

As it was mentioned in our previous papers [11,12], we use an effective value $\gamma = 2$ for the turbulence in weakly collisional tokamak plasmas instead of more conventional $\gamma = 5/3$. This empirical γ-value provides a better agreement with the large-aspect-ratio tokamak experiments [14,15]. In the cylindrical tokamak model the main radial force balance (quasi-equilibrium) described by Grad-Shafranov equation can be written in the following 1D form:

$$\frac{\pi}{U}\partial_r\left(\frac{r^2}{U}\right) + \partial_r p_0 + \pi\frac{qR}{U}\partial_r\left(\frac{qR}{U}\right) = 0, \qquad (1)$$

which allows us to calculate the function $U(r)$ directly. Here $q(r)$ is the conventional tokamak safety factor and r is the cylindrical radius. To avoid the complication caused by the additional calculation of the longitudinal current profile, we assume in the simulation that the profile $q(r)$ is fixed and specified by the condition $q(r) = q_0(1 + \alpha_q r^2)$, where the parameters q_0 and α_q are chosen for the corresponding experiment. The functions $p_0(t, r)$ and $U(t, r)$ can slowly vary in time due to the evolution of plasma equilibrium under the influence of transport processes.

Plasma fluctuations and turbulent velocity field are calculated in the frame of simple but self-consistent one-fluid MHD model. The adiabatic velocity field $\mathbf{v}_a(t,\psi,\varphi)$ obtained in [13] for general axisymmetric toroidal configurations with pure poloidal magnetic field has the form:

$$\mathbf{v}_a = \frac{c}{B_p^2}[\mathbf{B}_p \times \nabla\Phi(t,\psi,\varphi)] + c\mathbf{B}_p\lambda\partial_\varphi\Phi(t,\psi,\varphi) \sim \varepsilon\, c_s, \qquad (2)$$

where function $\Phi(t,\psi,\varphi)$ has a sense of 2D electric potential, function λ is defined in [13] and describes the velocity of adiabatic smoothing of pressure and density distributions along the field lines. $\lambda = 0$ in the cylindrical model, however, it logarithmically rises to infinity at the divertor separatrix. Small parameter ε determines level of fluctuations in the well-developed

turbulence and is defined by the following relation: $\varepsilon^3 \sim \chi / c_s a << 1$, where χ is a background local thermal diffusivity, c_s is the sound speed, and a is a minor radial scale.

E×**B** convection defined by Eq. (2) does not perturb the poloidal magnetic field and is formally unaffected by the toroidal magnetic field. The independence of convection on the toroidal field seems somewhat strange for tokamaks. Nevertheless we can argue, why the simplified model allows us to obtain reasonable results even in the case of tokamak. First of all let us mention that any LF quasi-electrostatic plasma convection in the axisymmetric systems with nested toroidal magnetic surfaces should not perturb the poloidal magnetic flux. From the other hand-side, independently on a presence of toroidal magnetic field $\mathbf{B}_T$ we can consider the function $\Phi(t,\psi,\varphi)$ as the potential in the equatorial cross-section (θ = 0) at the low-field side of the equivalent torus. The potential has to be almost flute-like even in the presence of $\mathbf{B}_T$ and can be approximately transformed as follows:

$$\Phi(t,\psi,\varphi) \quad \Rightarrow \quad \Phi(t,\psi,(\varphi - q(\psi)\theta)) \ . \tag{3}$$

Substituting the complete magnetic field $\mathbf{B} = \mathbf{B}_T + \mathbf{B}_p$ instead of $\mathbf{B}_p$ and the potential transformed in accordance with (3) into the expression (2) one can surprisingly find that the radial (normal to the surface) component of such modified $\mathbf{v}_a$ does not depend on $\mathbf{B}_T$:

$$\mathbf{v}_a \cdot \nabla\psi = \frac{c}{B^2}[\mathbf{B}\times\nabla\Phi(t,\psi,(\varphi - q(\psi)\theta))]\cdot\nabla\psi \equiv \frac{c}{B_p^2}[\mathbf{B}_p\times\nabla\Phi(t,\psi,\varphi)]\cdot\nabla\psi \ . \tag{4}$$

Of course, due to magnetic shear, the real potential is more complex function of coordinates, however, this circumstance cannot change the radial component of $\mathbf{v}_a$ appreciably. For these reasons we expect that our simplified dynamic model of plasma convection is able to provide reasonable values for the surface-averaged convective heat and particle fluxes.

In accordance with [13] the reduced equation of motion has the meaning of Euler-Lagrange equation corresponding to the adiabatic motion with velocity (2) and takes the form:

$$\partial_t\big|_\psi \hat{w} + [\Phi,\hat{w}] - \frac{1}{2}[\hat{\rho},\langle v_a^2\rangle] + \frac{1}{U^2}\partial_\psi U \partial_\varphi S = \{DT\}_w \ , \tag{5}$$

$$[\,\Phi\,,\,\hat{w}\,] \equiv \partial_\psi\Phi\,\partial_\varphi\hat{w} - \partial_\varphi\Phi\,\partial_\psi\hat{w} \ ,$$

where the time derivative is taken at fixed ψ, $\langle\ldots\rangle$ denotes the flux-tube-averaging procedure, and $\hat{w}$ is the canonical momentum of the adiabatic motion. It has the form

$$\hat{w} = \partial_\psi(\hat{\rho}\left\langle R^2\right\rangle\partial_\psi\Phi) + \partial_\varphi\left(\hat{\rho}\left\langle\frac{1}{R^2B^2} + \lambda^2B^2\right\rangle\partial_\varphi\Phi\right), \tag{6}$$

and can be named as the specific dynamic vorticity of plasma in a magnetic flux tube. R is the local value of the major toroidal radius (R = const in the cylindrical model). Eqs. (5) and (6) are written in terms of the following more adequate variables: the specific flux-tube volume $U(\psi)$, flux-tube-averaged entropy function $S = \langle p\rangle U^2$, and the mass of plasma particles in the flux-tube volume $\hat{\rho} = \langle\rho\rangle U$, which are introduced instead of the poloidal magnetic field B_p, total plasma pressure p, and the mass-density ρ respectively. These variables allow us to account explicitly the invariant properties inherent in the LF plasma dynamics (see [13] for details). The Eq. (5) is the exact consequence of the initial MHD equation of motion. The left-hand-side of this equation contains the terms describing the ideal plasma dynamics, while the right-hand-side denoted as $\{DT\}_w$ describes dissipative terms, which accounts a background kinematic viscosity η and contains the second-order spatial derivatives. Eq. (6) allows us to calculate the function Φ for known functions $\hat{w}$ and $\hat{\rho}$.

Reduced equations for S and $\hat{\rho}$ are obtained in [8,13] by means of flux-tube-averaging of initial continuity and heat transport equations and takes the following conservative form:

$$\partial_t\big|_\psi S + [\Phi, S] = \{DT\}_S\,, \qquad \partial_t\big|_\psi \hat{\rho} + [\Phi, \hat{\rho}] = \{DT\}_\rho, \tag{7}$$

where the right-hand-sides denoted as $\{DT\}_S$ and $\{DT\}_\rho$ again describe dissipative terms, which account a background thermal and particle diffusivities and contain the second-order spatial derivatives. Functions S and $\hat{\rho}$ consist of a surface-averaged slowly varying functions $S_0(t,\psi)$ and $\rho_0(t,\psi)$ and small fluctuating components $\tilde{S}(t,\psi,\varphi)$ and $\tilde{\rho}(t,\psi,\varphi)$:

$$S = \overline{S}(t,\psi) + \tilde{S}(t,\psi,\varphi), \quad \tilde{S} \sim \varepsilon^2 \overline{S}, \tag{8}$$

$$\hat{\rho} = \overline{\rho}(t,\psi) + \tilde{\rho}(t,\psi,\varphi), \quad \tilde{\rho} \sim \varepsilon^2 \overline{\rho}. \tag{9}$$

The function $S_0(t,\psi)$ is typically maintained near the marginally stable state: $|\nabla S_0| \sim \varepsilon^2 S_0 / a^2$. The final transport equations are obtained by φ-averaging of Eqs. (7) and allow us to calculate the slowly varying functions $S_0(t,\psi)$ and $\rho_0(t,\psi)$. Excluding these φ-averaged parts from the Eqs. (7) we obtain the equations for the fluctuating components $\tilde{S}(t,\psi,\varphi)$ and $\tilde{\rho}(t,\psi,\varphi)$. For the fluctuations with dominant spatial scales the dissipative terms in the right-hand-sides of equations (7) and (5) are of the order of ε^2 in comparison with the ideal terms in the left-hand-sides. However, these dissipative terms provide a suppression of fluctuations with sufficiently small-scales due to second-order spatial derivatives (see [13] for details).

One of the discussed regimes implies the presence of "sawtooth" oscillations. In this regime, the ECR heating is localized near the magnetic axis that results in a peaked pressure profile and induces the development of the internal kink mode, which leads to a fast flattening of the pressure profile in the central region bounded by q = 1 surface and to formation of a pressure jump near this surface. Since the internal kink mode is associated with the Alfvén type perturbations, it is not described by our simple turbulent model. However, we are interested not in sawtooth oscillations, but in their effect on the turbulent convection and transport in the region q >1. For this purpose we can use a simple model equation that describes the formation of pressure profile $p_0(t,r)$ in the region q < 1 in the presence of sawtooth oscillations. In terms of the dimensionless time discussed in Section 3, this equation can be written as follows:

$$\partial_t p_0(t,r) = \varepsilon^2 \frac{1}{r}\partial_r (rK\,\partial_r p_0(t,r)) + \frac{2}{3}(\varepsilon^2 Q_{st} + Q_{IK}(t,r))\,, \tag{10}$$

where K is an effective thermal diffusivity (for simplicity, we take K = const ~ r_c^2) and the energy source includes both the standard component $\varepsilon^2 Q_{st}$, which accounts the ECR and ohmic heating, and an additional component Q_{IK}, which is periodically (with a period of 40-50 dimensionless times) turned on for a short time to form the fast flattening of the pressure profile similarly to the internal kink.

3. Results of simulation

Self-consistent plasma convection and the resulting transport processes in the cylindrical plasma column were simulated as an evolutionary problem with given initial and boundary conditions. The initial conditions correspond to parameters of T-10 tokamak [14,15], more precisely to the parameters of shot #33965, in which the toroidal magnetic field was B_T = 2.5T, the major plasma radius was R = 150 cm, the minor plasma radius (restricted by the

limiter) was r_d = 30 cm, and the q = 1 surface had the radius $r_c \approx$ 10cm. The plasma density and the electron and ion temperatures at the axis were $n_0 = 6.23 \cdot 10^{13} \mathrm{cm}^{-3}$, T_{e0} = 2.075 keV, and T_{i0} = 0.767 keV, respectively. The plasma center was negatively charged with a typical radial potential difference $\Delta\Phi \approx$ 100V.

Under the assumption of zero fluctuations at the surface q =1 the total heat flux through this surface is determined only by the thermal diffusivity χ at $r = r_c$. According to the data of shot #33965, electrons and ions have almost the same effective χ values at the surface q = 1, and this value approximately corresponds to the ion neoclassical value. For this reason, we assume that the background thermal diffusivity χ has the neoclassical radial scaling with the value $\chi(r_c)$ = 0.9 m^2/s at the surface $r = r_c$. The dimensionless time unit (d.u.) in the simulations for T-10 corresponds approximately to 111 μs. The total energy source $Q_E(t,\psi)$ includes the ECR heating Q_{ECR}, ohmic heating Q_{OH}, viscous heating Q_{visc} due to turbulence dissipation, and radiative losses Q_{rad}. In the basic regime (a) of simulations, Q_{ECR} is the dominant part (80%) of the total power Q_E and is localized near the surface r_{h1} = 12.5 cm with the half-width of 2.5cm. The ohmic heating Q_{OH} is 20% of Q_E and is flatly distributed mainly in the region $r < r_c$. Radiative losses are 10% of the total power and increase parabolically towards the periphery.

Here we present the results of simulations for four different regimes. The basic regime (a) corresponds to the conditions of shot #33965. Regime (b) has the same initial conditions and the same total integral power input $\int (Q_{ECR} + Q_{OH}) r dr$, but 60% of the initial Q_{ECR} is switched closer to the plasma edge in a moment t = 100. Regime (c) illustrates fast transients in transport processes caused by the ECR turn on and the succeedent ECR turn off. Regime (d) illustrates the transport processes in the presence of sawtooth oscillations.

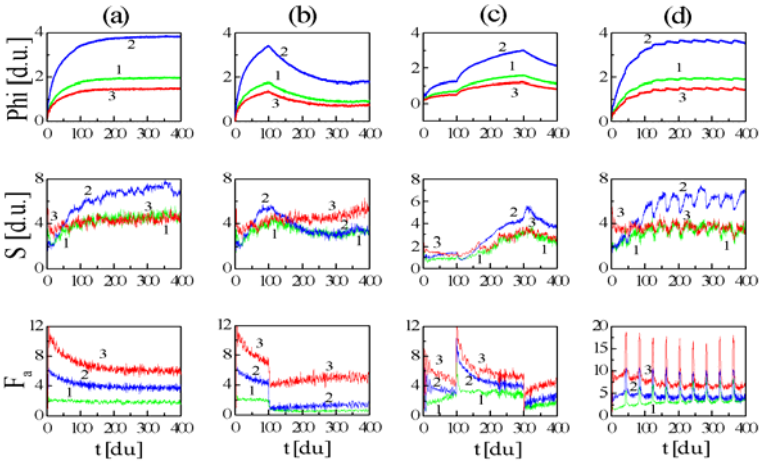

FIG.1. Evolution of fluctuations of potential Φ, entropy S, and anomaly factor F_a in regimes (a), (b), (c), and (d) at three surfaces: 1 - surface r_1 =13 cm; 2 - surface r_2 =20 cm; 3 - surface r_3 =27 cm.

FIG. 1 shows the evolution of surface-averaged fluctuations of potential Φ and entropy S (more precisely, square roots of surface-averaged square values of fluctuations $\left(\widetilde{\Phi^2}\right)^{1/2}$ and $\left(\widetilde{S^2}\right)^{1/2}$ in dimensionless units), as well as the anomaly factor $F_a = f^{an} / f^{ncl}$, which is the ratio of the total (anomalous) surface-averaged heat flux to the background (neoclassical) heat flux. FIG. 1a illustrates the basic regime (a). It is seen that the stage of linear instability and the initial formation of nonlinear turbulent structures transforms after $t \approx$20 (~2 ms) to a stage of well developed turbulence, which slowly evolves with a characteristic time comparable with

the energy lifetime $\tau_E \approx 29$ ms. Hereinafter, the energy lifetime is defined as the ratio of the integral plasma thermal energy to the total integral heating power. FIG. 1b presents regime (b) with the switching of 60% of Q_{ECR} to another gyrotron, which provides the ECR heating near r_{h2} = 25 cm with a half-width of 1.25 cm. After the ECR power redistribution, the anomaly factor F_a decreases sharply at all radii with a very short transient time Δt ~200÷300 μs, while the fluctuation levels decrease smoothly (with the typical time ~τ_E). This means that the convective heat flux varies primarily due to a fast change of phase between the fluctuations of $\tilde{\Phi}$ and $\tilde{S}$, rather than due to a decrease of the fluctuation level. In the core region (lines 1 and 2 in FIG. 1b), the anomaly factor F_a decreases even below 1 immediately after the ECR power redistribution and remains at low level later, while at the edge (at $r_3 > r_{h2}$) value F_a is maintained at a level comparable with the level in regime (a) (compare the lines 3 in FIG. 1a and 1b). FIG. 1c illustrates regime (c), in which the ECR power is turned on at r_{h1} = 12.5 cm in the moment t = 100 and then is turned off in the moment t = 300. Similar to regime (b), the fast reduction (enhancement) of F_a is seen at all radii after the corresponding ECR power changes. After the fast changes of F_a the plasma heating (cooling) processes in both scenarios proceed with characteristic times comparable with τ_E. Similar to the experiments, turbulence maintains and quickly recovers the pressure profile consistency after fast transients in all regimes with the modification of plasma heating. FIG. 2 shows the normalized pressure profiles at four moments of time before and after the central ECR heating turn on at t = 100. Crosses at FIG. 2 present the pressure profile in T-10 experiment. The normalized pressure profiles are almost unchanged in the region of well-developed plasma convection (for $r > 10$ cm) and correlate reasonably with the experimental profile, while the absolute values of pressure can differ in factor greater than 2 in different moments of time. Such behavior of heat transport is similar to that observed in T-10 experiments with ECH turn on/off. The reduction of F_a in regime (b) is consistent with the reduction of heat flux in ASDEX Upgrade experiments with the redistribution of ECR power (see FIG. 3 in [16]). T-10 also has appropriate gyrotrons to realize the regime (b).

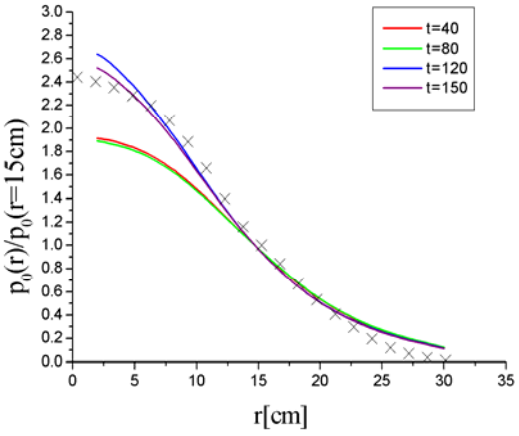

FIG. 2. Normalized pressure profiles at four moments of time before and after the central ECR heating turn on. Crosses correspond to T-10 experiment.

FIG. 1d illustrates the nonlocal response of fluctuations and transport processes in the region $q > 1$ to the presence of sawtooth oscillations. In this regime the ECR heating is localized in aria $r < 4$ cm near the magnetic axis. The pressure profile in the region $q < 1$ is formed in accordance with Eq. (10). Evolutions of potential Φ and entropy S fluctuations in regimes (d) and (a) are very similar, except for weak oscillations of S-fluctuation level at the frequency of sawtooth oscillations in regime (d). At the same time, the anomaly factor F_a in regime (d)

exhibits sharp bursts (almost doubling of F_a for a time of about 1ms). Bursts appear immediately after the flattening of the pressure profile in the region $q < 1$ and indicate that convection automatically rearranges to provide the fast transfer of heat pulse through the region $q < 1$ to the edge. This result is in agreement with numerous observations at tokamaks in the presence of sawtooth oscillations.

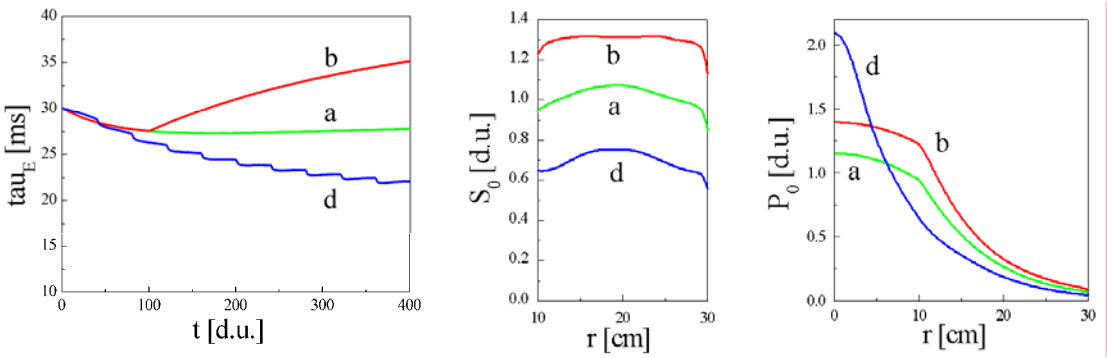

FIG.3. Evolution of plasma energy life-time τ_E and radial profiles of entropy function $S_0(r)$ and plasma pressure $p_0(r)$ in the moment t =400 in regimes (a), (b), (d).

FIG. 3 shows the evolution of the plasma energy lifetime τ_E and radial profiles of entropy function $S_0(r)$ and plasma pressure $p_0(r)$ in the three regimes (a), (b), and (d). Line (b) shows that the energy lifetime increases appreciably after the switching of 60% of the ECR power to the surface r_{h2} = 25 cm and exceeds the lifetime in regime (a) by 25% at t = 400. This result is slightly surprising for the traditional diffusion transport theory, but it is sufficiently natural for the discussed turbulent model, because the anomaly factor is significantly reduced in regime (b) in a wide radial range, whereas the turbulence level remains high enough to maintain the pressure profile near the turbulently relaxed state (see $S_0(r)$ profiles at FIG. 3). The switching of 60% of the ECR power to the edge seems to be sufficiently optimal, because the further increase in this power to 70% or higher leads to a flattening of the pressure profile in the central region and prevents the further increase in τ_E, despite the almost complete suppression of central turbulence. Regime (b) can be classified as a nonstandard L-H transition without the formation of an external transport barrier. Curve (d) shows that τ_E under central ECR heating decreases appreciably in comparison with the basic regime (a). In this case, if the volume of the region $q < 1$ is small, the direct influence of sawtooth oscillations on τ_E is not too strong and causes only small short-term drops in τ_E.

The radial profiles of entropy function $S_0(r)$ and plasma pressure $p_0(r)$ at the time t = 400 are also shown at FIG. 3. In all regimes the pressure profiles at $r < 10$ cm are calculated using Eq. (10). Only standard heating Q_{st} exists in regimes (a) and (b), whereas Q_{IK}, which imitates the internal kink, additionally exists in regime (c). The entropy profiles in the convective region 10 cm < r < 30 cm in all regimes are close to the turbulent-relaxed state $S_0(r) = \text{const}$, which can be considered as a condition of "pressure profile consistency" (criterion for a "canonical" profile) in our model. We remind that the correlation of calculated pressure profiles with the pressure profile measured in T-10 experiment is illustrated by FIG. 2. Entropy function has the highest value in the regime (b), in which it is the most close to the turbulent-relaxed profile $S_0(r) = \text{const}$. The pressure profile in regime (c) is represented immediately before the development of the internal kink. As a result of the central ECR heating, this profile is highly peaked near r = 0, but the total thermal plasma energy in this regime is lower than in regimes (a) and (b).

4. Summary

Relatively simple adiabatically-reduced fluid-like dynamical model is proposed to simulate the low-frequency turbulence and the resulting non-diffusive transverse plasma transport in the hot core region of tokamaks. The results of simulations have shown a rather good qualitative and quantitative agreement with a number of experiments. Evolutions of plasma turbulence and anomalous heat transport in tokamaks were simulated for four different regimes with ECR heating at times intervals those exceed the energy life-time. The turbulent convection in our simulations demonstrates the tendency to form the "pressure profile consistency", which are similar to that in T-10 experiments. Redistribution of 40-90% of the ECR power towards the plasma periphery significantly reduces turbulence and transverse heat transport. This result is consistent with the previous experiments at the ASDEX Upgrade and can be tested in experiments at T-10 and other tokamaks. Transport processes in regimes with turn on/off the ECR heating and in the presence of sawtooth oscillations have been simulated. The simulation results reproduce the fast changes in transport flows observed in many experiments.

The results obtained demonstrate efficiency of the proposed simple dynamic model for the simulations of LF turbulence and the resulting transport processes in the tokamak core plasmas. The developed approach is the most efficient for simulations of regimes with fast changes of plasma heating and confinement conditions. Our model is predictive and can be used for analysis and optimization of future tokamak experiments.

We are grateful to N.A. Kirneva, Yu.N. Dnestrovskii, and K.A. Razumova for stimulating discussions. The work was fulfilled (partly) in the framework of realization of the Federal program "Scientific and pedagogical personnel of innovative Russia" for 2009-2012 and by Grant 65382.2010.2 for support of Leading Scientific Schools in Russian Federation.

References

[1] WADE, M. R. and DIII-D Team, Nucl. Fusion **47** (2007) S543.
[2] TAKENAGA, H. and JT-60 Team, ibid. **47** (2007) S563.
[3] GRUBER, O. for the ASDEX Upgrade team, ibid. **47** (2007) S622.
[4] YAMADA, H., et al., ibid. **45** (2005) 1684.
[5] MOTOJIMA, O., et al., ibid. **47** (2007) S668.
[6] CHO, T., et al., Phys. Rev. Letters **97** (2006) 055001.
[7] CHO, T., et al., Phys. Plasmas **15** (2008) 056120.
[8] PASTUKHOV, V.P., and CHUDIN, N.V., Plasma Phys. Reports **27** (2001) 907.
[9] PASTUKHOV, V.P., and CHUDIN, N.V., JETP Letters **82** (2005) 356.
[10] PASTUKHOV, V.P., and CHUDIN, N.V., Transactions of Fusion Science and Technologies **51** (2007) 34.
[11] PASTUKHOV, V.P., and CHUDIN, N.V., *Proceedings of the 22nd IAEA Fusion Energy Conference* (Geneva, 2008), TH/P8-26.
[12] PASTUKHOV, V.P., and CHUDIN, N.V., JETP Letters **90** (2009) 651.
[13] PASTUKHOV, V.P., Plasma Phys. Reports **31** (2005) 577.
[14] RASUMOVA, K.A., et al., Plasma Phys. Control. Fusion **48** (2006) 1373.
[15] RASUMOVA, K.A., et al., ibid. **50** (2008) 105004.
[16] RYTER, F., et al., Nucl. Fusion **43** (2003) 1396.